Dynamic Aspects of Lattice Inclusion Complexation Involving a Phase Change. Equilibrium, Kinetics, and Energetics of Guest-Binding to a Hydrogen-Bonded Flexible Organic Network

Takehisa Dewa,[†] Ken Endo,[†,‡] and Yasuhiro Aoyama*[,†,‡]

Contribution from CREST, Japan Science and Technology Corporation (JST), and Institute for Fundamental Research of Organic Chemistry, Kyushu University, Hakozaki, Higashi-Ku, Fukuoka 812-8581, Japan

Received April 13, 1998

Abstract: The solid/gas complexation of anthracenebisresorcinol host (**1**) and ethyl acetate as a guest was monitored by pressure-decay, X-ray powder diffraction, and gravimetric/calorimetric thermal desorption analyses. It involves an exothermic (∼30 kcal/mol) phase transition and exhibits "vertical" adsorption as well as desorption "isotherms" at a threshold (equilibrium) pressure (P_{th}) of the guest vapor. This is in accord with the phase rule for a two-component/three-phase/one-freedom system. The activation energies of adsorption and desorption are 2.3 and 34 kcal/mol, respectively; desorption at 25 °C takes weeks. The crystal structure of the ethyl acetate adduct illustrates how the flexible hydrogen-bonded network of host **1** adjusts itself to the small guest. Other polar guests (ester, ketone, and alcohol) behave similarly and give rise to desorption-resistant stable adducts, except for the least bulky members of the ester and ketone guests, i.e., methyl acetate and acetone. The mechanism of phase transition is discussed in light of the lack of size effect as for the host and well-behaved guest-prebinding at $P < P_{th}$.

Introduction

There has been much recent interest in organic and metal−organic network materials whose guest-binding properties are reminiscent of traditional zeolites.[1] Lattice inclusion compounds have so far been studied mostly from the static viewpoint (stoichiometry, crystal structure, selectivity, etc.) on recrystallized host−guest adducts.[2] In the context of zeolite analogues, it is also essential to know how preformed solid hosts interact with the guests.

Scattered information is available as to guest-removal, -addition, and -exchange properties of many host systems,[1b−f] including the bisresorcinol derivative of anthracene (**1**, Chart 1).[1g,3] Upon recrystallization, host **1** forms stoichiometric (2:1 in most cases) guest−host adducts (eq 1, G = guest), where guest molecules (●) are included in each cavity maintained by the hydrogen-bonded (O−H···O−H) network of the host (structure **2**, where dotted lines represent hydrogen bonds, Chart 1). Volatile guests can be removed upon heating the adducts, to give polycrystalline guest-free apohost. The apohost subsequently binds various guests not only as liquids or gases but also, in some cases, as solids (eq 1) in the same guest−host stoichiometry as in recrystallization. The resulting adducts exhibit the same X-ray powder diffractions as the corresponding single-crystalline samples. Guest exchange also occurs. This gives a basis of the novel catalysis by the present host in the solid state.[4]

$$\mathbf{1} + n\mathrm{G} \overset{K}{\rightleftharpoons} \mathbf{1}\cdot n\mathrm{G} \quad (1)$$

$$\mathrm{CaO} + \mathrm{CO_2} \overset{K}{\rightleftharpoons} \mathrm{CaCO_3} \quad (2)$$

Selected host−guest complexations have been studied from the kinetic and thermochemical viewpoints.[5] In addition, solid-

[†] CREST.

[‡] Kyushu University.

(1) For examples of recent work, see: (a) Russell, V. A.; Evans, C. C.; Li, W.; Ward, M. D. *Science* **1997**, *276*, 575−579. (b) Brunet, P.; Simard, M.; Wuest, J. D. *J. Am. Chem. Soc.* **1997**, *119*, 2737−2738. (c) Yaghi, O. M.; Davis, C. E.; Li, G.; Li, H. *J. Am. Chem. Soc.* **1997**, *119*, 2861−2868. (d) Kondo, M.; Yoshitomi, T.; Seki, K.; Matsuzaka, H.; Kitagawa, S. *Angew. Chem., Int. Ed. Engl.* **1997**, *36*, 1725−1727. (e) Gardner, G. B.; Kiang, Y.-H.; Lee, S.; Asgaonkar, A.; Venkataraman, D. *J. Am. Chem. Soc.* **1996**, *118*, 6946−6953. (f) Ung, A. T.; Gizachew, D.; Bishop, R.; Scudder, M. L.; Dance, I. G.; Craig, D. C. *J. Am. Chem. Soc.* **1995**, *117*, 8745−8756. (g) Endo, K.; Sawaki, T.; Koyanagi, M.; Kobayashi, K.; Masuda, H.; Aoyama, Y. *J. Am. Chem. Soc.* **1995**, *117*, 8341−8352. (h) Kolotuchin, S. V.; Fenlon, E. E.; Wilson, S. R.; Loweth, C. J.; Zimmerman, S. C. *Angew. Chem., Int. Ed. Engl.* **1995**, *34*, 2654−2657. (i) Subramanian, S.; Zaworotko, M. J. *Angew. Chem., Int. Ed. Engl.* **1995**, *34*, 2127−2129. (j) Goldberg, I.; Krupitski, H.; Stein, Z.; Hsiou, Y.; Strouse, C. E. *Supramol. Chem.* **1995**, *4*, 203−221. (k) Fujita, M.; Kwon, Y. J.; Washizu, S.; Ogura, K. *J. Am. Chem. Soc.* **1994**, *116*, 1151−1152. (l) Abrahams, B. F.; Hoskins, B. F.; Michail, D. M.; Robson, R. *Nature* **1994**, *369*, 727−729. (m) Reddy, D. S.; Goud, B. S.; Panneerselvam, K.; Desiraju, G. *J. Chem. Soc., Chem. Commun.* **1993**, 663−664. (n) Kaszynski, P.; Friedli, A. C.; Michl, J. *J. Am. Chem. Soc.* **1992**, *114*, 601−620. (o) Ermer, O.; Lindenberg, L. *Helv. Chim. Acta* **1991**, *74*, 825−877. (p) Miyata, M.; Shibakami, M.; Chirachanchai, S.; Takemoto, K.; Kasai, N.; Miki, K. *Nature* **1990**, *343*, 446−447. (q) Weber, E.; Hecker, M.; Csöregh, I.; Crugler, M. *J. Am. Chem. Soc.* **1987**, *111*, 7866−7872.

(2) (a) Zimmerman, S. C. *Science* **1997**, *276*, 543−544. (b) *Comprehensive Supramolecular Chemistry*; Lehn, J.-M., Atwood, J. L., Davies, J. E. D., MacNicol, D. D., Vögtle, F., Eds.; Pergamon Press: Oxford, 1996; Vol. 6. (c) *Inclusion Compounds*; Atwood, J. L., Davies, J. E. D., MacNicol, D. D., Eds.; Oxford University Press: Oxford, 1991. (d) Bishop, R. *Chem. Soc. Rev.* **1996**, *25*, 311−319. (e) Zaworotko, M. J. *Chem. Soc. Rev.* **1994**, *23*, 283−288. (f) *Molecular Inclusion and Molecular Recognition—Clathrates I and II. Topics in Current Chemistry*; Weber, E., Ed.; Springer-Verlag: Berlin-Heidelberg, 1987 and 1988; Vols. 140 and 149.

(3) (a) Kobayashi, K.; Endo, K.; Aoyama, Y.; Masuda, H. *Tetrahedron Lett.* **1993**, *34*, 7929−7932. (b) Aoyama, Y.; Endo, K.; Kobayashi, K.; Masuda, H. *Supramol. Chem.* **1995**, *4*, 229−241. (c) Aoyama, Y.; Endo, K.; Anzai, T.; Yamaguchi, Y.; Sawaki, T.; Kobayashi, K.; Kanehisa, N.; Hashimoto, H.; Kai, Y.; Masuda, H. *J. Am. Chem. Soc.* **1996**, *118*, 5562−5571.

S0002-7863(98)01245-1 CCC: $15.00
Published on Web 08/20/1998

Chart 1

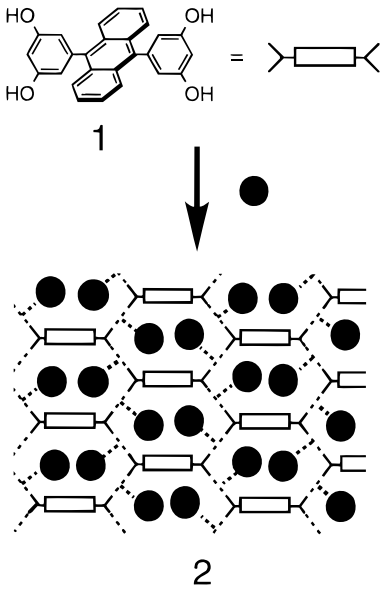

state reactions constitute an important area of organic synthesis.[6] Despite such phenomenologically rich information, we are still far away from a thorough understanding of how solid-state complexation takes place. For example, how is the organic solid−gas complexation (eq 1, G = gaseous guest) similar to or different from inorganic solid−gas reactions such as that shown in eq 2? There are a number of fundamental questions which are related to each other. (1) Do the solid host and its solid adduct share the same phase or constitute different phases? (2) Do guest-binding cavities maintained by an organic network survive[7] or collapse upon guest-removal? (3) How do guest molecules diffuse in the solid host?

The object of the present work is to get an overview of lattice inclusion complexation from dynamic viewpoints. We report here on the equilibrium and kinetic/energetic properties of a guest-induced organic phase transition phenomenon.

Results

Binding Isotherms. The complexation of apohost **1** (∼150 mg) with gaseous ethyl acetate (eq 1, $n = 2$) was followed by monitoring the pressure change in the sealed gas phase. A binding isotherm is shown in Figure 1, where molar ratios of guest bound to host used are plotted (○) against guest pressure (P, in Torr) at 25 °C for the adsorption (→; up to ∼90% of the saturation vapor pressure (P_s) of the guest) and desorption (←; down to ∼5% of P_s) processes upon computer-controlled stepwise addition or removal of the guest vapor. Each point represents a state where the change in pressure in a fixed waiting time of 300 s (5 min) has become smaller than 1% of the pressure at that point ($\Delta P < 0.01P$). Under these *fast-scanning* conditions, desorption of included guests is too slow to be recorded. Adsorption is much faster. Figure 2 shows how pressure decays from point a ($P = 16.3$ Torr) to b ($P = 16.2$ Torr) in Figure 1 upon addition of 6 Torr of the guest vapor at point a. This relaxation takes ∼80 min, and the whole measurement of the isotherm (○) requires 21 h.

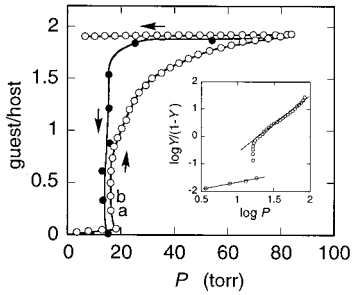

Figure 1. Binding isotherms for gaseous ethyl acetate with powdered apohost **1** at 25 °C under the fast-scanning (○) or the slow-scanning (●) conditions. The adsorption curve under the slow-scanning conditions is very similar to the fast-scanned one (○). Inset: Hill plot for the adsorption curve (○).

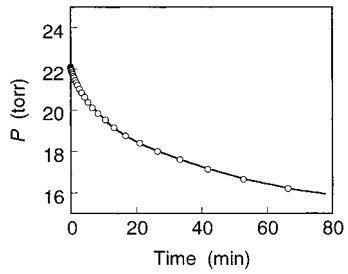

Figure 2. Time course of adsorption-based pressure decay from point a to b (Figure 1) for the solid−gas complexation of host **1** and ethyl acetate at 25 °C.

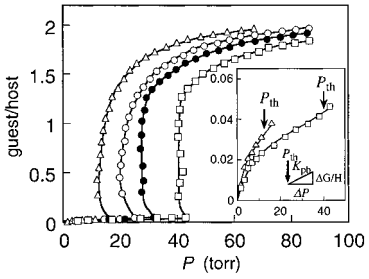

Figure 3. Adsorption isotherms for ethyl acetate with nonpulverized pieces of apohost **1** under the fast-scanning conditions at 20 (△), 25 (○), 30 (●), and 35 °C (□). Inset: expansion of the $P \leq P_{th}$ regions for selected (at 20 and 35 °C) isotherms; K_{pb} is the slope at $P = P_{th}$.

When, however, a much longer waiting time of 9999 s (2.8 h) is admitted, desorption is clearly observed, as shown by the closed circles in Figure 1. The adsorption curve, not shown for clarity, remains similar to the fast-scanned one (○). Each drop in the desorption curve under these *slow-scanning* conditions takes ∼1 week, and the whole isotherm (●) requires 7 weeks to be recorded. The vertical desorption line almost overlaps with the adsorption line at guest/host <1, with practically no hysteresis. These must represent an equilibrium binding curve.

There is no notable size dependence for the host. The isotherms in Figure 1 are for powder samples of apohost. That for nonpulverized large ($3 \times 3 \times 3$ mm^3) crystals as an apohost sample under the fast-scanning conditions at 25 °C is shown in Figure 3, together with those at other (20, 30, and 35 °C) temperatures. An apparent size independence has been observed for other hosts.[1e] The catalytic activity of host **1** also shows little size dependence.[4a]

Threshold Points and Binding Rates. The adsorption curve is characterized by a sharp threshold point (P_{th}, Figure 3 and

(4) (a) Endo, K.; Koike, T.; Sawaki, T.; Hayashida, O.; Masuda, H.; Aoyama, Y. *J. Am. Chem. Soc.* **1997**, *119*, 4117−4122. (b) Sawaki, T.; Endo, K.; Kobayashi, K.; Hayashida, O.; Aoyama, Y. *Bull. Chem. Soc. Jpn.* **1997**, *70*, 3075−3079.

(5) Caira, M. R.; Nassimbeni, L. R. In ref 2b, Chapter 25.

(6) Toda, F. In ref 2b, Chapter 15.

(7) Some metal−organic networks are robust enough to withstand the removal of included guests.[1c−e] Recent studies indicate that this is also the case for some hydrogen-bonded networks.[1b,f]

Table 1. Threshold Pressures and Rate and Binding Constants for the Complexation of Host **1** with Ethyl Acetate at Various Temperatures

T (K)	P_{th} (Torr)[a]	$10^3 K$ (torr^{-2})[b]	$10^2 k_{ad}$ (min^{-1})[c]	$10^3 K_{pb}$ (torr^{-1})[d]	k_{pt} (torr·min^{-1})[e]
293	12	6.8	2.9	1.4	20
298	20	2.4	3.1	1.2	27
303	28	1.3	3.3	1.0	32
308	40	0.6	3.5	0.8	42
ΔH or E	[kcal mol^{-1}][f]	−29[g]	2.3[h]	−6.2[i]	8.6[j]

[a] Threshold pressure (see footnote 8). [b] $K = 1/P_{th}^2$. [c] Adsorption-based pressure decay rate constant in reference to eq 3. [d] Approximate prebinding constant at $P = P_{th}$ in reference to the inset of Figure 3. [e] $k_{pt} = k_{ad}/K_{pb}$; phase-transition rate constant. [f] Refer to Figure 7. [g] ΔH_{ad}. [h] E_{ad}. [i] ΔH_{pb}. [j] E_{pt}.

Table 1)[8] and consists of three parts: the vertical region at $P \cong P_{th}$, a milder follow-up region at $P > P_{th}$, reaching a saturation guest/host ratio of 2, and a prebinding region at $P \leq P_{th}$, where a small fraction of guest (guest/host $\leq$ 0.04) is bound.[9] The threshold pressures (P_{th}) become lower at lower temperatures (Table 1).

In the inset of Figure 1 is shown the Hill plot,[10] which is often used to describe cooperative or allosteric binding processes in homogeneous solutions. The three parts mentioned above are characterized by different slopes. The vertical one at $P \cong P_{th}$ indicates a remarkably cooperative nature of the guest-binding at this region. It may be more important, however, that this treatment of the binding data according to a homogeneous host−guest complexation fails to give a linear correlation for the whole pressure range.

The three regions also show different kinetic responses. The point-to-point pressure decay is much faster at $P \leq P_{th}$[9] or $P > P_{th}$ than that at $P \cong P_{th}$, where pressure decays as shown in Figure 2. This decay curve fits with the first-order relaxation kinetics (eq 3; P_e is the resulting "equilibrium" pressure). The

$$-d(P - P_e)/dt = k_{ad}(P - P_e) \qquad (3)$$

derived rate constant of $k_{ad} = 3.1 \times 10^{-2}$ min^{-1} holds for all the point-to-point decays in the vertical or the $P \cong P_{th}$ region. It is also remarkable to note that there is practically no dependence of the rate constant on whether the apohost used has been pulverized or not. Thus, the guest-binding rate at this region is dependent neither on the progress of complexation nor on the size of the apohost sample. The corresponding rate constants at various temperatures are summarized in Table 1. They show a slightly positive temperature dependence; an activation energy of $E_{ad} = 9.5$ kJ/mol (2.3 kcal/mol) for the adsorption of ethyl acetate is obtained as the slope of the Arrhenius plot of ln k_{ad} vs $1/T$.[11]

Specific Surface Area and Crystal Structures. The apohost is obtained upon heating in vacuo of single crystals of ternary host−guest adduct **1**·2($CH_3CO_2CH_2CH_3$)·2(C_6H_6).[3b] It is polycrystalline and shows two bands of ν_{O-H} in the IR spectrum, a broad one at 3370 cm^{-1} and a sharper one at 3510 cm^{-1}, which are assignable to the hydrogen-bonded and free OH groups (O−H···O−H), respectively. All attempts to obtain single crystals of apohost were unsuccessful.

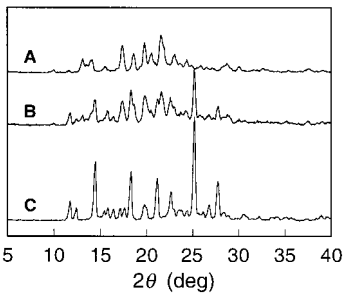

Figure 4. X-ray powder diffraction patterns for apohost **1** (A), an apparent 1:1 adduct, **1**·$CH_3CO_2CH_2CH_3$ (B), and a fully packed 2:1 adduct, **1**·2($CH_3CO_2CH_2CH_3$) (C).

The specific surface area of apohost was estimated by the BET analysis (Figure I of Supporting Information) of the adsorption of N_2 at 77 K; $A_{BET} = 7$ m^2/g. This is 2 orders of magnitude smaller than the typical values of $A_{BET} = 500-700$ m^2/g for zeolites A or molecular sieves. The BET results and IR evidence thus suggest that the apohost forms a condensed phase with more or less collapsed cavities while basically maintaining intermolecular hydrogen bonds.

The ethyl acetate adduct **1**·2($CH_3CO_2CH_2CH_3$) ($\nu_{O-H} = 3400$ cm^{-1} and $\nu_{C=O} = 1689$ cm^{-1}) obtained by the gas adsorption (eq 1, $n = 2$) exhibits the same powder X-ray diffractions (Figure 4C) as the corresponding single crystals. It thus recovers a microscopic single-crystal structure of the adduct. Controlled adsorption of the guest (Figure 1) affords adducts **1**·x($CH_3CO_2CH_2CH_3$) having various apparent guest/host ratios of $0 < x < 2$. Their powder diffractions are represented as a weighed sum of those of apohost (Figure 4A) and 2:1 (guest to host) adduct **1**·2($CH_3CO_2CH_2CH_3$) (Figure 4C), as shown for an apparent 1:1 adduct, **1**·$CH_3CO_2CH_2CH_3$, in Figure 4B as an example. As far as powder diffractions are concerned, it is a 1:1 mixture of two domains, guest-free apohost and fully packed 2:1 adduct.

The crystal structure of single-crystalline adduct **1**·2($CH_3CO_2CH_2CH_3$) is shown in Figure 5A. As is well documented, the host forms a hydrogen-bonded (O−H···O−H) 2D network (side view a; $l_a = 14.03$ Å and $l_c = 4.80$ Å) but in a somewhat different manner from the previous cases.[1g,3] It forms a folded molecular sheet with partial overlap of the anthracene rings (top view b of the sheets), and neighboring sheets are parallel aligned; $l_s = 8.85$ Å. The ethyl acetate guests (green) are hydrogen-bonded to one sheet (O−H···O−H···O═C), with their methyl and ethoxy groups extending into the adjacent ones. Figure 5B shows, for comparison, the crystal structure of the ternary adduct **1**·2($CH_3CO_2CH_2CH_3$)·2(C_6H_6), having additional benzene guests (yellow) as a space-filler ($l_a = 14.27$ Å, $l_c = 9.88$ or 9.95 Å, and $l_s = 7.05$ or 7.25 Å). It is characterized in the following way.[3a] (1) The long axes of the anthracene rings are perpendicular to the sheet so that there is no overlap of the anthracene moieties. (2) Two ethyl acetate molecules are accommodated in each intrasheet cavity. (3) The sheets are layered in a staggered manner. (4) Two benzene molecules occupy the space left, one in the cavity and the other between sheets. All the so-far investigated 2:1 adducts, having relatively bulky guests such as alkyl benzoate[3b] and benzophenone,[1g] have crystal structures in lattice pattern B. The present crystal structure in pattern A is quite atypical in this respect.

(8) Due to overloading at the $P \leq P_{th}$ region, pressure often drops upon addition of more guest at $P \cong P_{th}$. In such a case, the pressure immediately after the pressure drop is taken as P_{th}.

(9) The guest molecules bound in this region undergo ready desorption, even under the fast-scanning conditions, when pressure is swept backward immediately after reaching P_{th}.

(10) The Hill equation, $\log[Y/(1 - Y)] = n \log P + \log K$, holds for the equilibrium (eq 1) when host **1** and adduct **1**·nG share a common phase, as in homogeneous solution, where Y ($0 < Y < 1$) is the extent of complexation.

(11) Kinetics of a number of solid−gas complexations at constant P and T have been studied by the gravimetric methods. For example, a diol−acetone complexation exhibits a threshold pressure (P_{th}); the binding rates at $P > P_{th}$ show a linear dependence on P and an anti-Arrhenius (i.e., smaller rates at higher temperatures) behavior (Barbour, L. J.; Caira, M. R.; Nassimbeni, L. R. *J. Chem. Soc., Perkin Trans. 2* **1993**, 2321−2322).

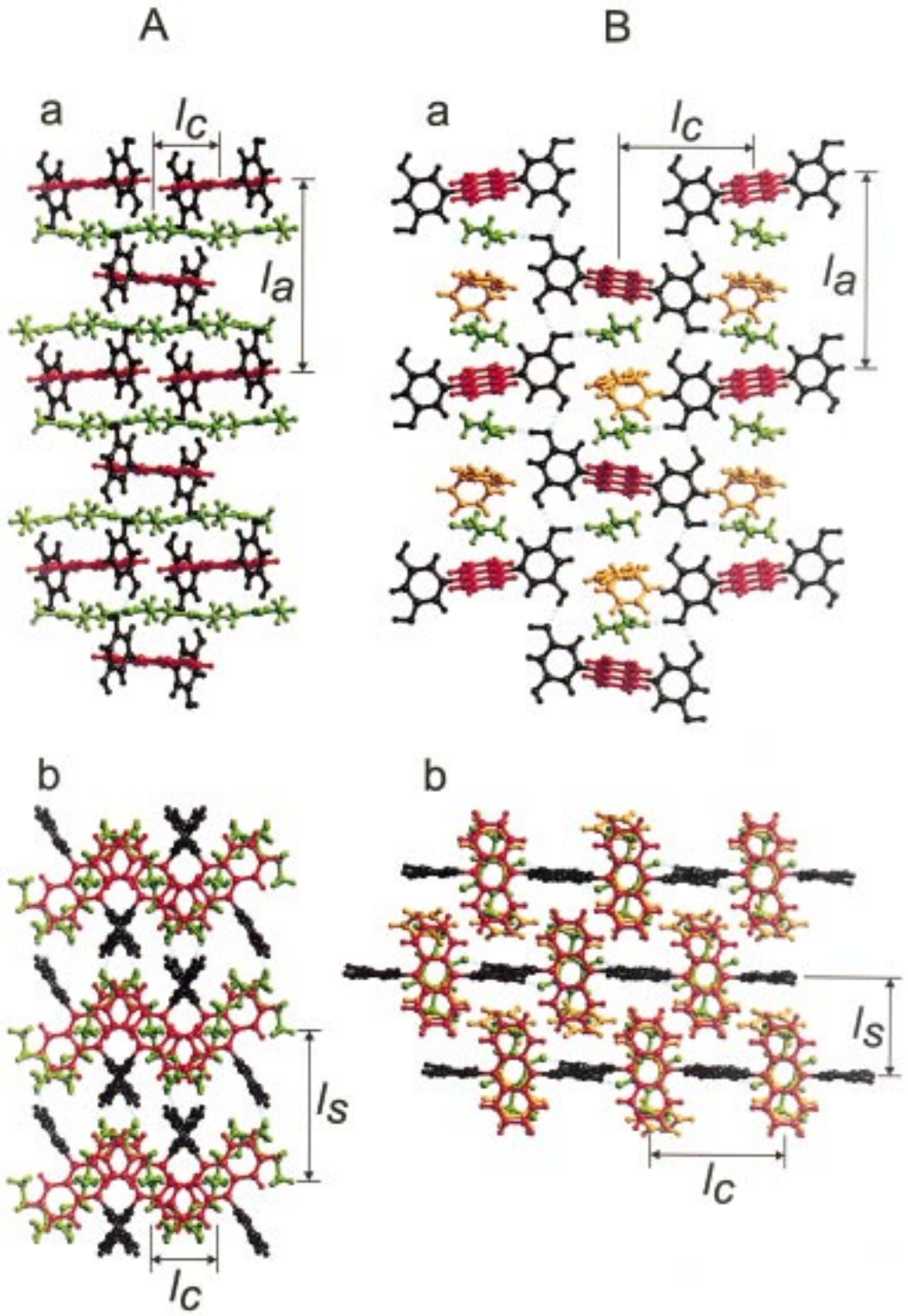

Figure 5. Crystal structures of adducts **1**·2($CH_3CO_2CH_2CH_3$) (A) and **1**·2($CH_3CO_2CH_2CH_3$)·2(C_6H_6) (B); side view of a molecular sheet constructed by a hydrogen-bonded network of the host (a) and top view of three adjacent sheets (b). l_a, l_c, and l_s are inter-ring, intercolumn, and intersheet distances, respectively. The anthracene rings, resorcinol rings, ethyl acetate, and benzene are shown in red, black, green, and yellow, respectively.

Desorption and Energetics. Desorption of included guests can be monitored by thermogravimetry (TG) and differential scanning calorimetry (DSC) or thermal analysis (DTA).[5] Figure 6A shows the TG (solid line) and DTA (dashed line) thermograms for the ethyl acetate adduct at a heating rate of $\beta = 20$ °C/min. The loss in weight upon heating the adduct corresponds to the weight of included guests. The accompanying endothermicity corresponds to a heat of desorption of $\Delta H_{de} = 128$ kJ/mol (31 kcal/mol). The resulting apohost is stable up to 350 °C and then gradually decomposes. The adsorption/desorption cycles can be repeated many times without causing any notable change in the binding isotherms, powder diffraction patterns, or thermograms (TG/DTA or DSC).

The activation energy of desorption (E_{de})[12] is estimated by recording TG curves at various heating rates (β) and by plotting log β vs $1/T$ at a given extent of desorption,[13] according to the relation $\log \beta = -0.4567E_{de}/RT + \text{constant}$. At 50% desorption, $T = 51.6$ (324.6), 58.9 (331.9), 61.2 (334.2), 63.7 (336.7), and 65.1 °C (338.1 K) at $\beta = 1$, 3, 5, 7, and 10 °C/min; $E_{de} =$ 144 kJ/mol (34 kcal/mol) as obtained from the slope of the log

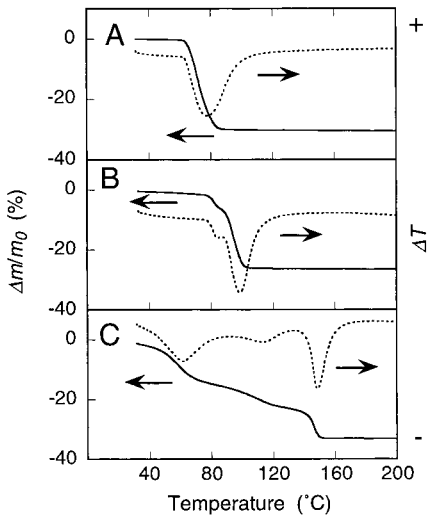

Figure 6. TG (solid line) and DTA (dashed line) thermograms for the ethyl acetate (A), methyl ethyl ketone (B), and 2-propanol (C) adducts at a heating rate of $\beta = 20$ °C/min. The samples prepared by gas adsorption were used after a fast scan of desorption at 25 °C; accurate compositions in the starting adducts are **1**·1.9($CH_3CO_2CH_2CH_3$) (cf. Figure 1, ○), **1**·2.7($CH_3COCH_2CH_3$) (curve b in Figure 8B), and **1**·3.8[$(CH_3)_2CHOH$] (curve c in Figure 8C). $\triangle T = T_{sample} - T_{reference}$ for the DTA thermograms are in arbitrary unit. The magnitudes of endothermic peaks for different guests cannot be compared.

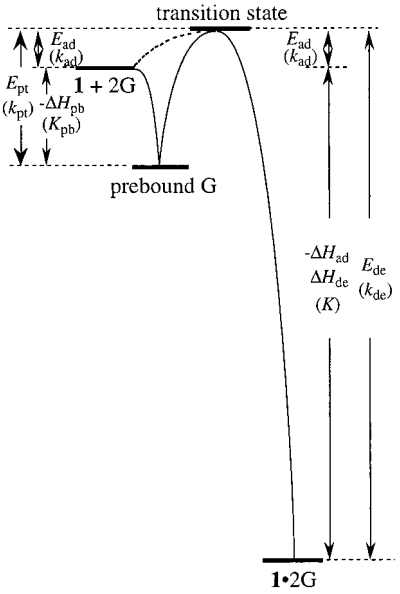

Figure 7. Schematic energy diagram for the solid−gas complexation of host **1** with gaseous ethyl acetate (eq 1, $n = 2$ and G = ethyl acetate). Definitions are as follows: k_{ad} and E_{ad} are the rate constant and activation energy of guest adsorption, k_{de} and E_{de} are the rate constant and activation energy of guest desorption, K and $\triangle H_{ad}$ ($\triangle H_{de}$) are the equilibrium constant and heat of guest adsorption (desorption), K_{pb} and $\triangle H_{pb}$ are the equilibrium constant and heat of guest prebinding, and k_{pt} and E_{pt} are the rate constant and activation energy of phase transition for prebound guest.

β vs $1/T$ plot. The heat of desorption (ΔH_{de})[12] and the activation energy of adsorption have been obtained above; $\Delta H_{de} = 128$ kJ/mol (31 kcal/mol) and $E_{ad} = 9.5$ kJ/mol (2.3 kcal/mol). Thus, an expected relationship of $E_{de} = \Delta H_{de} + E_{ad}$ is nicely met. In Figure 7 is shown a schematic energy diagram for the adsorption/desorption of ethyl acetate.

The enormous value of E_{de} predicts, on the basis of $d(\ln k_{de})/d(1/T) = -E_{de}/R$, a remarkable difference in desorption rate

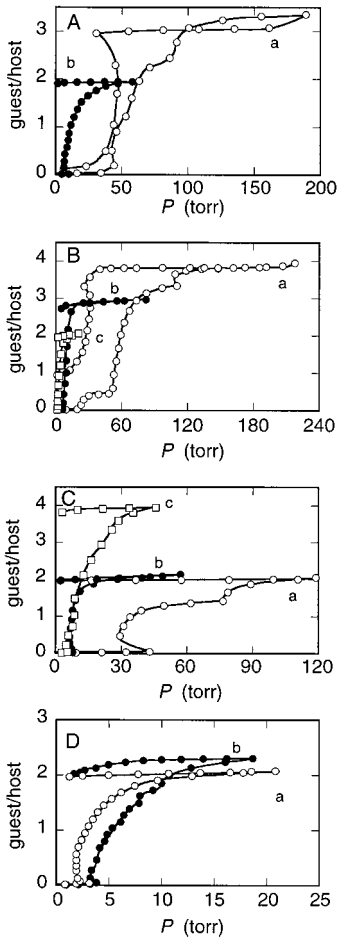

Figure 8. Binding isotherms for gaseous guests with apohost **1** at 25 °C under the fast-scanning conditions: A, methyl acetate (○) and isopropyl acetate (●); B, acetone (○), methyl ethyl ketone (●), and diethyl ketone (□); C, methanol (○), ethanol (●), and 2-propanol (□); D, propanol (○) and *sec*-butanol (●).

constants at 70 °C (343 K) and at 25 °C (298 K); $k_{de}^{343}/k_{de}^{298} \cong 2000$. This is consistent with the observed temperature dependence of desorption. Under the TG/DTA conditions with $\beta = 20$ °C/min, desorption starts at 62 °C and is complete at 86 °C (Figure 6A). It thus takes ∼1 min. Under the slow-scanning conditions at 25 °C, the point-to-point desorption along the vertical desorption line (●) in Figure 1 takes ∼1 week. If the half-lives of desorption at 70 °C (343 K) and 25 °C (298 K) are 1 min and 2 days, respectively, the rate ratio is $k_{de}^{343}/k_{de}^{298} \cong 3000$.

Binding Properties of Other Guests. In Figure 8A−D are shown the binding isotherms for other esters (methyl acetate and isopropyl acetate), ketones (acetone, methyl ethyl ketone, and diethyl ketone), and alcohols (methanol, ethanol, 2-propanol, propanol, and *sec*-butanol (2-butanol)), respectively, obtained under the fast-scanning conditions with a waiting time of 300 s. The essential features are similar to those for ethyl acetate.

(12) The thermal properties of inclusion compounds of diol hosts have been studied in detail. See, for example: (a) References 5 and 11. (b) Barbour, L. J.; Caira, M. R.; Coetzee, A.; Nassimbeni, L. R. *J. Chem. Soc., Perkin Trans. 2* **1995**, 1345−1349. (c) Caira, M. R.; Coetzee, A.; Nassimbeni, L. R.; Weber, E.; Wierig, A. *J. Chem. Soc., Perkin Trans. 2* **1995**, 281−284. (d) Bourne, S. A.; Nassimbeni, L. R.; Niven, M. L.; Weber, E.; Wierig, A. *J. Chem. Soc., Perkin Trans. 2* **1994**, 1215−1222. (e) Barbour, L. J.; Caira, M. R.; Nassimbeni, L. R. *J. Chem. Soc., Perkin Trans. 2* **1993**, 1413−1414. (f) Bourne, S. A.; Nassimbeni, L. R.; Toda, F. *J. Chem. Soc., Perkin Trans. 2* **1991**, 1335−1341.

(13) (a) Flynn, J. H.; Wall, L. A. *J. Polym. Sci., Part B* **1966**, *4*, 323−328. (b) Ozawa, T. *Bull. Chem. Soc. Jpn.* **1965**, *38*, 1881−1886.

Table 2. Pressures and Guest/Host Ratios at Threshold Points and at Saturation for the Complexation of Host **1** with Various Guests at 25 °C[a]

	R in CH_3CO_2R			R^1, R^2 in $R^1R^2C{=}O$			R in ROH				
guest[b]	Me	Et	*i*Pro	Me, Me	Me, Et	Et, Et	Me	Et	Pr	^{i}Pr	^{s}Bu
P_{th} (torr)[c]	44	20	6	20	7	2	30	7	2	5	3
$(guest/host)_{th}$[d]	0.04	0.04	0.02	0.02	0.02	0.02	0.05	0.02	0.04	0.04	0.05
P_s (torr)[e]	217	97	61	231	91	35	127	59	21	45	18
$(guest/host)_s$[f]	3	2	2	4	3	2	2	2	2	4	2

[a] Nonpulverized host was used for most measurements. [b] Me = methyl, Et = ethyl, Pr = propyl, ^{i}Pr = isopropyl, ^{s}Bu = *sec*-butyl. [c] Threshold pressure (see footnote 8). [d] Guest/host ratio at $P = P_{th}$. [e] Saturation vapor pressure. [f] Saturation guest/host stoichiometry expressed as an integer number after a fast scan of desorption.

The threshold pressures (P_{th})[8] for related guests follow a decreasing order of methyl > ethyl > isopropyl > *sec*-butyl with respect to the alkyl groups involved (Table 2). This trend indicates that, in the present series, bulkier guests show higher affinities.[14] A careful inspection of the isotherms at $P \leq P_{th}$ reveals that, despite a big span in P_{th}'s, the guest/host ratios at $P = P_{th}$ are rather constant at $(guest/host)_{th} = 0.02-0.05$ for all the guests (Table 2).

The guest/host stoichiometry at saturation binding is $(guest/host)_s = 2$ for most guests (Table 2), as in the case of recrystallization.[3b,c] Some (small) guests exhibit higher ratios, as was observed for acetone in the solid−liquid complexation;[3c] guest/host = 3 for methyl acetate (curve a in Figure 8A) and methyl ethyl ketone (b in 8B) and 4 for acetone (a in 8B) and 2-propanol (c in 8C) (Table 2). It is also noteworthy that the adsorption of methanol (a in 8C), methyl acetate, acetone, or 2-propanol occurs in a stepwise manner, although other (bulkier) guests show apparently monophasic adsorption isotherms at $P \geq P_{th}$.

The lack of desorption under the present fast-scanning conditions is also a common feature shared by most of the guests. The exceptions are the least bulky members of esters and ketones, i.e., methyl acetate and acetone, which readily lose ~3 molecules of included guest (Figure 8A and B, curve a).

The TG and DTA thermograms are shown in Figure 6B and C for methyl ethyl ketone and 2-propanol, respectively, as representative ketone and alcohol guests. Their desorption (Figure 6) and adsorption curves (Figures 1 and 8) are closely related to each other. Methyl ethyl ketone has a prepeak in both adsorption (b in 8B) and desorption (6B). When adsorption occurs in a stepwise manner, as in the case of 2-propanol (c in 8C), the corresponding desorption curve (6C) becomes stepwise, too.

Discussion

Phase Transition. The specific surface area of apohost ($A_{BET} = 7$ m^2/g) indicates that it is by no means porous. The powder diffraction studies show that apohost and its adduct have different diffractions and do not merge upon mixing. The thermal guest-removal from an adduct exhibits a well-behaved endothermicity. There is no doubt that the present apohost−adduct interconversion involves a phase transition. The phase rule for the equilibrium between three phases (two solid phases for apohost and adduct and one gaseous phase for guest) consisting of two components (host and guest) leaves one degree of freedom, i.e., $f = c - p + 2 = 2 - 3 + 2 = 1$. If, for example, temperature as the sole variable is fixed, the corresponding equilibrium pressure would also be automatically fixed. Thus, the pressure would be maintained during the adsorption/desorption process until one of the solid phases is completely consumed. This is what the rule says and is what was actually observed, as shown by the vertical adsorption and desorption (●) profile at $P \cong P_{th}$ under the slow-scanning conditions (Figure 1).

Such being the case, the threshold pressure (P_{th}) represents the equilibrium pressure for eq 1 ($n = 2$, G = ethyl acetate) and the equilibrium constant is expressed as $K = 1/P_{th}^2$. The temperature dependence of P_{th} (Table 1) allows us to evaluate the associated enthalpy change. The plot of $\ln K = -2 \ln P_{th}$ vs $1/T$, according to $d \ln K/d(1/T) = -\Delta H_{ad}/R$, yields a straight line, whose slope leads to $\Delta H_{ad} = -119$ kJ/mol (−29 kcal/mol) for this reaction (eq 1). This is in fairly good agreement with the DSC-determined value of $\Delta H_{de} = 128$ kJ/mol (31 kcal/mol).

For all the guests, curvature actually occurs for the adsorption profile at higher guest/host ratios ($P > P_{th}$). It remains to be elucidated whether this is due to continuous formation of new phases or due to a kind of phase fusion for the apohost and the adduct.

Mechanistic Implication. There are a number of relevant observations which shed light on the mechanism of the present phase transition. (1) The first-order pressure-decay kinetics (eq 3) indicates that the phase transition is driven by an excess guest pressure. (2) The phase transition is a *bulk* phenomenon, since the associated guest-binding rates are little affected by pulverization of the host. (3) The phase transition at $P \cong P_{th}$ is preceded by a reversible[9] prebinding region at $P \leq P_{th}$, having a curved or saturation-like isotherm (inset of Figure 3), where the guest/host ratios at $P = P_{th}$ are rather constant at 0.02−0.05 for all the guests (Table 2).

Items 1 and 3 suggest that there is a maximal *tolerable* amount of prebound guest, i.e., $(guest/host)_{th}$, and, upon overloading at $P > P_{th}$, the excess amount is *expelled* as host−guest adduct into a new phase. In reference to the inset of Figure 3, the excess amount ($\Delta G/H$) may be expressed as $\Delta G/H = K_{pb}\Delta P$, where K_{pb} is the approximate prebinding constant obtained as the slope of the isotherm ($P \leq P_{th}$) at $P = P_{th}$ and $\Delta P = (P - P_{th})$ is excess guest pressure. The rate of phase transition would be proportional to $\Delta G/H$, i.e., $-d(P - P_{th})/dt = k_{pt}K_{pb}(P - P_{th})$. Comparison of this with eq 3 ($P_e \cong P_{th}$) indicates that $k_{ad} = k_{pt}K_{pb}$. The prebinding constants (K_{pb}) and the phase-transition rate constants ($k_{pt} = k_{ad}/K_{pb}$) are summarized in Table 1, together with the associated enthalpy change and activation energy in reference to the energy diagram shown in Figure 7. Their compensating temperature dependencies make the overall adsorption process (k_{ad}) rather insensitive to temperature.

Another question is where prebinding of guest occurs. A logical site is the surface of the apohost. Such being the case, the curved prebinding isotherm (inset of Figure 3) represents a Langmuir-type surface adsorption, and the rate constant k_{pt} may be related to diffusion of surface-adsorbed guests. An alterna-

(14) The threshold pressures (P_{th}) for different guests are roughly correlated with boiling points of the guests. When P_{th}'s are plotted as a function of heats of condensation of the guests as vapors, different types of guests (esters, ketones, and alcohols) give separate correlation lines.

tive mechanism involves formation of a host−guest solid solution. In this case, the curvature of the prebinding profile reflects a deviation from Henry's law for an ideal solution, while k_{pt} stands for the rate of phase separation of the *oversaturated* solute (guest). The experimental observations seem to favor the solid−solution mechanism. First of all, this *bulk* mechanism, but hardly the surface mechanism, is consistent with the lack of size or pulverization effects (item 2 above). Pulverization of a solid may increase the surface area but keeps the volume unchanged. Second, the maximal tolerable amount of guest (guest/host = 0.04 for ethyl acetate at $P = P_{th}$) may sound reasonable as a solubility. It is, however, an unreasonably big number for monolayer surface coverage. It corresponds to the formation of at least seven layers of closely packed 2D guest sheet on the host, having a specific surface area of $A_{BET} = 7$ m^2/g.[15] Third, the smooth and progress-independent time course of the phase transition seems to be more compatible with the bulk/separation mechanism rather than the surface/diffusion mechanism. If the latter is operative, all the surface of the host would be covered by the adduct phase at an early stage, leaving no free surface of apohost exposed to the guest vapor.

Flexibility and Induced-Fit Adjustment. Host **1** forms various adducts with different guests.[16] There is a common feature in their crystal structures; they are composed of layers of hydrogen-bonded 2D sheets. It is remarkable that the adducts have similar packing efficiencies despite a big span in the size of included guests. Host **1** has three potential origins of flexibility with respect to the molecular structure (rotation around the anthracene-resorcinol axis), intermolecular interaction (simple or one-point O−H···O hydrogen bonds),[17] and network dimensionality (self-assembling 2D sheets). Figure 5 illustrates how the network adjusts itself to the size of the guest. Ethyl acetate is not big enough to be incorporated in lattice pattern B. The host molecules rotate, either clockwise or counterclockwise, around the hydrogen-bonded polyresorcinol axis (···O(H)−R−OH···O(H)−R−OH···O(H)−R−OH···; R = anthracenyl-C_6H_3) as a spine or a hinge to allow partial overlap of the anthracene rings in pattern A. The intramolecular folding of the sheet, which results in a significant shortening of the intercolumn distance (l_c), is compensated by an elongation of the intersheet distance (l_s). Due to such an accordion-like intrasheet/intersheet adjustment, even the small ethyl acetate guest is well-packed in the adduct ($d = 1.28$, as compared with $d = 1.31$ for the benzophenone adduct[1g])[18] and the complexation is much more exothermic ($-\Delta H_{ad} \cong \Delta H_{de} \cong 30$ kcal/mol) than expected for a simple host−guest hydrogen-bond of the present type (C═O···H−O, $-\Delta H \leq 5$ kcal/mol).

There is a dramatic difference in desorption abilities between the least bulky guests (methyl acetate and acetone) and their next higher homologues (ethyl acetate and methyl ethyl ketone). The former (curve a in Figure 8A and B), but not the latter, readily desorbs, even under the fast-scanning conditions. These results, when coupled with an atypical crystal structure of the ethyl acetate adduct discussed above, suggest that (1) the bulkiness of a guest plays a crucial role and (2) the latter two are the smallest guests to which the present host network is adjustable. In other words, the former guests (methyl acetate and acetone) may be too small to be covered and stabilized by the network. In this connection, it is interesting to note that, in the enone−cyclohexadiene Diels−Alder reactions, the present host acts as a true turnover catalyst only for the least bulky enone, i.e., acrolein.[4a] Through these arguments, we see a strained and potentially porous nature of the apohost.

Concluding Remarks

This work shows how equilibrium is attained for a lattice inclusion phenomenon. Referring to the questions raised in the Introduction, these may be summarized as follows.

(1) The organic solid−gas complexation shown in eq 1, like an inorganic counterpart (eq 2), involves a phase transition, and its equilibrium state is best described in terms of a phase equilibrium for which the phase rule for an $f = 1$ system is applicable, except for the later part of the adsorption curve. It is not appropriate to treat or interpret such a system in terms of host−guest association in a single phase. Even the phrase "binding isotherm" may be misleading; only where $f \geq 2$, i.e., $c - p \geq 0$ can one define a binding isotherm describing how the extent of complexation changes with pressure (concentration) of the guest at equilibrium. One has to be careful also when interpreting the selectivity in guest-binding under competitive conditions, since different guests likely lead to different phases when incorporated in the host.

(2) There seems to be little objection to the argument that the present apohost **1** and its adduct constitute different phases because the former cannot sustain guest-free cavities. What happens, then, when a robust host can do this? It remains to be verified if, in such a case, the apohost with vacant cavities and its adduct indeed share a common phase so as to behave as an $f = 2$ system.

(3) One often wonders how guest molecules diffuse in the nonporous interior of a host, where complexation does occur. The complexation actually involves a phase transition, which is a bulk phenomenon. A more essential question would be how many guest molecules coherently diffuse out to form a new phase.

Finally, it may be interesting to note that the flexible network has dual roles. On one hand, it is adjustable to various guests, while keeping the basic network topology unchanged. On the other hand, it shows a sharp on/off response to the pressure of each guest. Such a property may suggest potential utilities of the present type of flexible hosts as selective separators of guest mixtures[19] and also as coherent materials, such as on/off devices.

Experimental Section

Apohost **1** was prepared as described, i.e., by removing the guest molecules from single-crystalline adduct **1**·2($CH_3CO_2CH_2CH_3$)·2(C_6H_6) of size (1−3)^3 mm^3 at 150 °C in vacuo.[3b] It was used either as obtained without pulverization or powdered after being ground in a mortar.

The binding isotherms were obtained with a BELSORP 18 automated gas adsorption apparatus. In the sample chamber (∼15 mL) maintained at 25.0 ± 0.1 °C was placed apohost **1** (∼150 mg), which had been

(15) $l = S_G/A_{BET}$, where l is the number of layers in concern, $A_{BET} = 7 \times 10^{20}$ Å^2/g of host, and the total area of the threshold amount of guest forming a closely packed monolayer is $S_G = (6 \times 10^{23})(1/M)(\text{guest/host})_{th}s_G$ (in Å^2), in which the occupation area of a molecule of ethyl acetate guest is estimated to be $s_G = 25$ Å^2 on the basis of its density (0.8) as a liquid.

(16) Adducts whose crystal structures have been determined include **1**·2G (G = ethyl acetate (this work), alkyl benzoate (alkyl = methyl, ethyl, propyl, isobutyl),[3b] dialkyl ketone (alkyl = propyl, butyl, pentyl),[1g] benzophenone,[1g] or citronellal[4b]), **1**·2G·G′ (G = ethyl acrylate and G′ = 1,3-cyclohexadiene),[4a] and **1**·2G·2G′ (G = ethyl acetate and G′ = benzene[3a] or G = water and G′ = *p*-xylene (unpublished result)). The calculated densities of these adducts fall in the range of $d = 1.1-1.3$.

(17) Rigid polyol hosts such as steroidal bile acid derivatives[1p] (Miyata, M.; Sada, K. In ref 2b, Chapter 6) and chiral bicyclic diols[1f, 2d] (Bishop, R. In ref 2b, Chapter 4) show dynamic guest-binding properties more or less similar to those observed here.

(18) Competitive cocrystallization experiments indicate that ketone and ester guests R^1R^2C═O show highest affinities to host **1** when the chain length of R^1 and R^2 is 4, as in the case of 5-nonanone and propyl or isobutyl benzoate.[1g] Benzophenone is also such a 4,4-ketone.

(19) Furusho, Y.; Aida, T. *J. Chem. Soc., Chem. Commun.* **1997**, 2205−2206.

pretreated at 150 °C at $<10^{-3}$ Torr for 6 h just prior to use. The larger gas chamber (176.36 mL) with a pressure gauge was kept at 50.0 ± 0.1 °C. Helium gas at a certain pressure was introduced in the gas chamber and was allowed to diffuse into the sample chamber by opening a valve. The change in pressure allowed an accurate determination of the volume of the total gas phase. Host−guest complexation was monitored in a similar manner by using a guest vapor in place of helium. The amount of guest adsorbed was calculated readily from the pressure difference ($P_{cal} - P_e$), where P_{cal} is the calculated pressure if there were no guest adsorption, as in the case of helium, and P_e is the observed equilibrium pressure, at which the change in pressure in 300 s (fast scanning) or 9999 s (slow scanning) had become smaller than 1% of the pressure at that point. All operations were computer-controlled and automatic.

The specific surface areas (A_{BET}) of apohost were obtained by using the same apparatus. The adsorption isotherm for N_2 at 77 K (Figure I of Supporting Information) fit well with the BET equation, $P_e/V(P_s - P_e) = 1/V_mC + [(C - 1)/V_mC](P_e/P_s)$, where P_s is the saturation vapor pressure of N_2 at 77 K and is 760 Torr, V (mL/g) is the amount (in terms of volume in the standard state) of N_2 adsorbed per gram of adsorbent, V_m is that for saturation monolayer coverage, and C is a constant. Two unknowns, $V_m = 1.61$ mL/g and $C = 236$, were determined from the slope and intercept of the linear BET plot (inset of Figure I, Supporting Information) of $P_e/V(P_s - P_e)$ vs P_e/P_s in the monolayer adsorption range of $P_e/P_s = 0.05-0.30$. The specific surface area of $A_{BET} = 7$ m^2/g was then evaluated according to $A_{BET} = (V_m/22400)N_Aa_m$, where N_A is Avogadro's number and a_m is the occupation area of a molecule of N_2 and is 0.162 nm^2, or $0.162/10^{18}$ m^2.

All thermal measurements were performed by using a Seiko Denshi TG/DTA 220U and DSC 220U thermal analysis system with a computer-controlled data acquisition and analysis system. Each sample (∼5 mg), obtained by the gas adsorption method, was loaded on an Al open-sample pan under the stream of nitrogen (300 mL/min). TG/DTA thermograms were recorded at a heating rate of $\beta = 20$ °C/min or, for the ethyl acetate adduct, at slower rates ($\beta = 1-10$ °C/min) for kinetic purposes. DSC thermograms were taken at $\beta = 5$ °C/min, and the heats of desorption were calibrated by using indium as a reference.

X-ray powder diffractions were obtained with a Shimadzu XD-D1w X-ray diffractometer. The crystal structure of adduct **1**·2($CH_3CO_2CH_2CH_3$) was determined with a Rigaku AFC7R four-cycle diffractometer with Mo Kα ($\lambda = 0.710\ 69$ Å) radiation as described in previous papers;[1g,3] $C_{34}H_{34}O_8$ (570.64), monoclinic, $P2_1/n$, colorless, $a = 12.847(1)$ Å, $b = 9.579(3)$ Å, $c = 13.343(1)$ Å, $\beta = 115.24(1)°$, $V = 1485.2(4)$ Å^3, $Z = 2$, $d = 1.276$ g/cm^3. Intensity data were collected at 20 °C using the $\omega-2\theta$ scan technique to $2\theta_{max} = 55°$ and were corrected for both Lorentz and polarization effects. The structure was solved by direct methods SIR92 and refined anisotropically for nonhydrogen atoms; $R = 0.039$, $R_w = 0.063$, and GOF = 1.46.

Acknowledgment. This work was supported by CREST (Core Research for Evolutional Science and Technology) of the Japan Science and Technology Corp. and also by a grant-in-aid for COE Research "Design and Control of Advanced Molecular Assembly Systems" (No. 08CE2005) from the Ministry of Education, Science, and Culture, Japan.

Supporting Information Available: Figure I (binding isotherm for N_2 at 77 K and derived BET plot) and crystal parameters and tables of crystal structural data with thermal ellipsoidal figure including atomic coordinates and B_{iso}/B_{eq}, anisotropic displacement parameters, bond lengths, bond angles, torsion angles, and nonbonded contacts out to 3.60 Å for adduct **1**·2($CH_3CO_2CH_2CH_3$) (9 pages, print/PDF). X-ray crystallographic files, in CIF format, are available on the Internet only. See any current masthead page for ordering information and Web access instructions.

JA9812453